

118826

UNCLASSIFIED
~~CONFIDENTIAL~~
LEVEL II

MOST Project
03042

OOVI LIBRARY COPY

OOVI B1

001846

NWC

1

ADAO 67138

A NEW ABSORPTION COEFFICIENT EXPRESSION
FOR USE IN
SONAR RANGE PREDICTION

Good.

(12) 37p.

(1) H. R. HALL & W. H. WATSON
(NWC)

DDC FILE COPY

(11) 10 Apr 67

DDC
RECEIVED
APR 9 1967
F

DISTRIBUTION STATEMENT A
Approved for public release;
Distribution Unlimited

The opinions and assertions contained here-
in are the private ones of the writer, and
are not to be considered as official, or as
reflecting the views of the Department
of the Navy or the Navy at large.

DOWNGRADED AT 3-YEAR INTERVALS
DECLASSIFIED AFTER 12 YEARS
DOD, DMR 5200.10

~~CONFIDENTIAL~~
UNCLASSIFIED

COPY NO. 1

001846

205

~~CONFIDENTIAL~~

UNCLASSIFIED

03042

ABSTRACT

↙ Several different expressions are available for the absorption coefficient of sound in seawater. This study has resulted in an improved absorption loss coefficient expression for use in sonar range prediction. Computations were carried out to determine the errors which might result from the use of the alternative absorption coefficient expressions. It is demonstrated that significant differences in the predicted detection range can occur when inexact expressions are used.



ACCESSION for		
NTIS	White Section	<input checked="" type="checkbox"/>
EDG	Diff Section	<input type="checkbox"/>
UNANNOUNCED		<input type="checkbox"/>
JUSTIFICATION <i>Per letter on file</i>		
BY		
DISTRIBUTION/AVAILABILITY CODES		
Doc.	AVAIL.	and/or SPECIAL
A		

REVERSE SIDE BLANK

~~CONFIDENTIAL~~

UNCLASSIFIED

INTRODUCTION:

A number of different empirical expressions exist for the calculation of α , the absorption coefficient of sound in seawater. A careful investigation of the various expressions and the data upon which they are based was undertaken to determine which of these expressions appears to be most nearly "correct," and, in any case, to choose or develop a single expression for use in sonar range-prediction calculations. It was felt that the final expression should: (1) be reasonably simple, (2) have corrections for variations in temperature, pressure, and salinity, and (3) have some basis of validity in experimental measurements.

REVIEW AND ANALYSIS OF EXISTING EXPRESSIONS:

Four of the best-known expressions for α have been selected for study. [1, 2, 3, 4] These expressions are listed below:

Marsh and Schulkin ^[1]

$$\alpha_A = \left(\frac{.018587s f_t^2}{f^2 + f_t^2} + \frac{.026847f^2}{f_t} \right) \cdot (1 - 6.54 \times 10^{-4} P) \text{ dB/kyd} \quad (1)$$

where

$$f_t = 21.9 \times 10^{(6t+118)/(t+273)} \text{ kc/s}$$

f = frequency in kc/s

P = pressure in atmospheres

s = salinity in parts per thousand

t = temperature in °C.

Thorp ^[2]

$$\alpha_B = .0542 f^{1.5} \text{ dB/kyd} \quad (2)$$

Sheehy and Halley ^[3]

$$\alpha_C = .033 f^{1.5} \text{ dB/kyd} \quad (3)$$

Leroy ⁽⁴⁾

$$\alpha_D = .00549 \cdot f^2 + \frac{.241 f^2}{2.89 + f^2} \text{ dB/kyd} \quad (4)$$

The value of α as a function of frequency was computed using the above expressions. These computations were carried out for average deep water values of temperature, salinity, and pressure. The resulting curves have been plotted in figure 1, where we have also included a summary of experimental data points originally presented by Thorp.*

It may be noted that although all curves are in fair agreement at high frequencies the curves of Sheehy and Halley, and Marsh and Schulkin conform more closely to the experimental points. The curve of Thorp tends to fall slightly above the experimental data for these higher frequencies. At low frequencies the curves of Thorp, and Sheehy and Halley fall fairly close to the experimental data, whereas the curve of Marsh and Schulkin falls considerably below the experimental data. The curve of Leroy confirms the general magnitude of the other curves, and represents a general overall shape which is consistent with the data presented.

Whether the expressions considered predict values of attenuation or of absorption (i. e., dissipation) is a moot point, which only further experimental and theoretical investigations can answer. It is worth noting that Leroy's measurements ⁽⁴⁾ were made over relatively short, direct paths (≤ 40 KM). Since his measurements support the "excess" low frequency loss predicted by Thorp, and Sheehy and Halley, they tend to dispel the theory that scattering or other non-dissipative loss from long-range deep sound channels is responsible for the excess. Of the other explanations for the excess attenuation at low frequencies, none seems to have won wide-spread acceptance.

*At the time of publication it was brought to the authors' attention by Mr. Thaddeus G. Bell, USNUSL, that Thorp has an unpublished, modified expression which fits the data more closely near the 3.5 kc/s region.

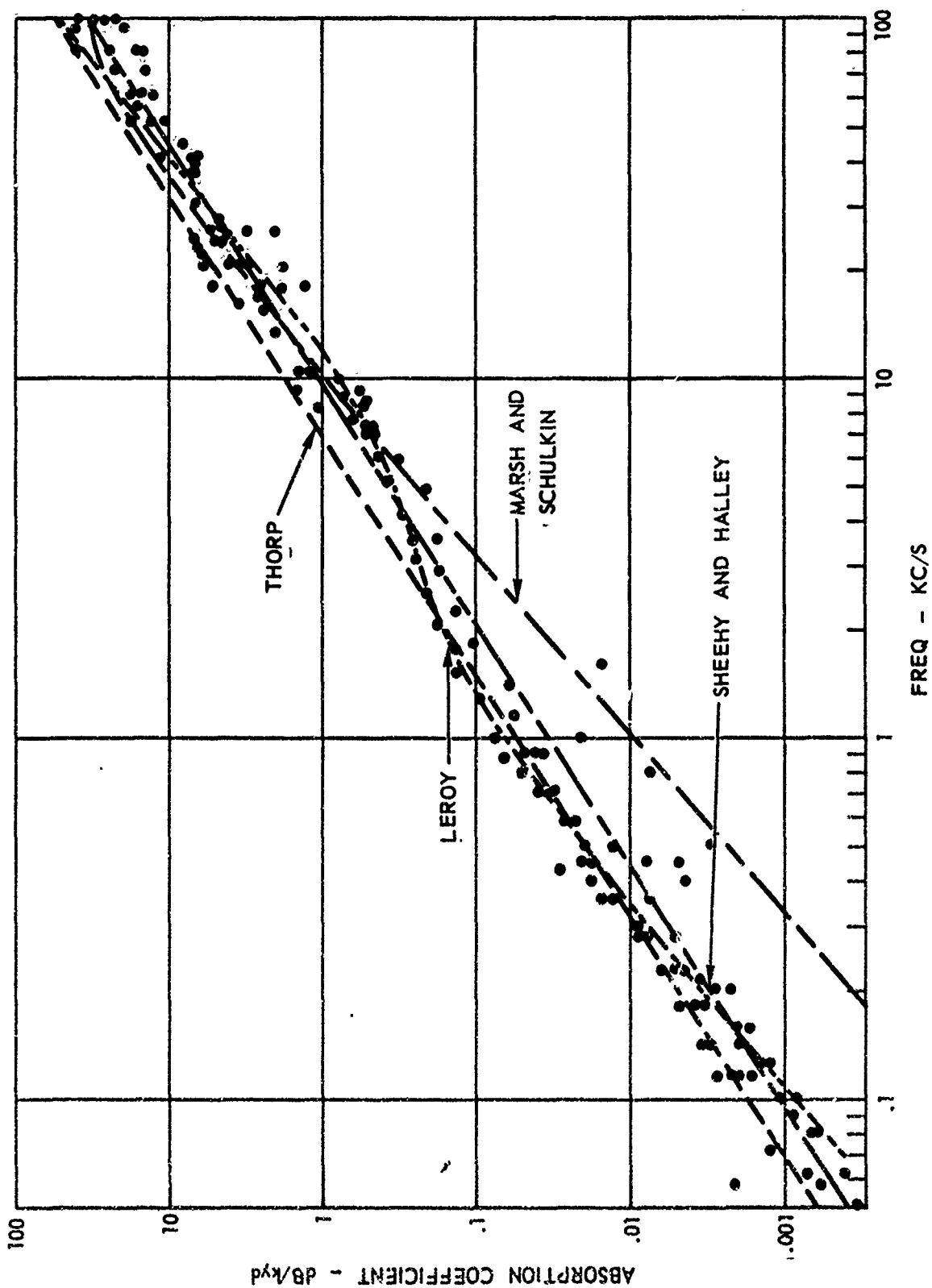


Figure 1. Comparison of Absorption Coefficients, Temperature = 40° F, Salinity = 35‰, pressure = 125 ATM.

CONFIDENTIAL

For the purposes of range prediction it is desirable to have a single expression for absorption coefficient which will give a good approximation to the available data, and will also include the effects of temperature, salinity, and pressure when these effects are important.

The expression of Marsh and Schulkin includes effects of temperature, salinity, and pressure, but it is a very poor fit to all low frequency data. The expressions of Thorp, Sheehy and Halley, and Leroy give reasonably good correlation with the data at the lower frequencies, but do not include the effects of temperature, salinity and pressure.

It is therefore concluded that no one expression, of those available, is suitable for use at all frequencies; however, a combination of two of the expressions does appear to be optimum. In the following section, the expressions of Thorp, and Marsh and Schulkin will be combined mathematically into a single, continuous expression for use at all practical sonar operating frequencies and under variable environmental conditions.

PROPOSED EXPRESSION FOR ABSORPTION COEFFICIENT:

It is proposed that the new expression for absorption coefficient have the form:

$$\alpha = B_L \cdot \alpha_B + B_H \cdot \alpha_A, \quad (5)$$

where α_B and α_A represent the expressions of Thorp, and of Marsh and Schulkin respectively, and B_L and B_H represent frequency-dependent weighting factors.

It is required that α_B be the dominant term at low frequencies, and that α_A be the dominant term at high frequencies, with a smooth transition between the two. Thus, B_L should be maximum at low frequencies and monotonically decreasing with increasing frequency, while B_H should have the opposite frequency dependence.

These requirements suggest that a low-pass filter transfer function be used for B_L , and the complementary high-pass filter

CONFIDENTIAL

transfer function be used for B_H . Of the many transfer functions available, the pair chosen for B_L and B_H are of the maximally-flat amplitude (Butterworth) type: [5]

$$\left. \begin{aligned} B_L &= \frac{1}{1 + \left(\frac{f}{3.2}\right)^3} \\ B_H &= \frac{1}{1 + \left(\frac{3.2}{f}\right)^3} \end{aligned} \right\} \quad (6)$$

When $f = 3.2$ kc/s (the cross-over frequency), $B_L = B_H = 1/2$. At $f = 0$, $B_L = 1$ and $B_H = 0$, while at $f = \infty$, $B_L = 0$ and $B_H = 1$. The sum of B_L and B_H is unity at all frequencies. B_L and B_H are shown as functions of frequency in figure 2.

The desired expression for attenuation coefficient is obtained by combining eqs. (1), (2), (5), and (6). After simplification, this gives:

$$\alpha = \frac{1.7760f^{1.5}}{32.768 + f^3} + \left(\frac{1 - 6.54 \times 10^{-4} P}{1 + 32.768/f^3} \right) \quad (7)$$

$$\left(\frac{.018587s f_t^2}{f^2 + f_t^2} + \frac{.026847f^2}{f_t} \right) \quad \text{dB/kyd}$$

where, as before,

$$f_t = 21.9 \times 10^{(6t+118)/(t+273)} \text{ kc/s}$$

f = frequency in kc/s

P = pressure in atmospheres

s = salinity in parts per thousand

t = temperature in °C.

CONFIDENTIAL

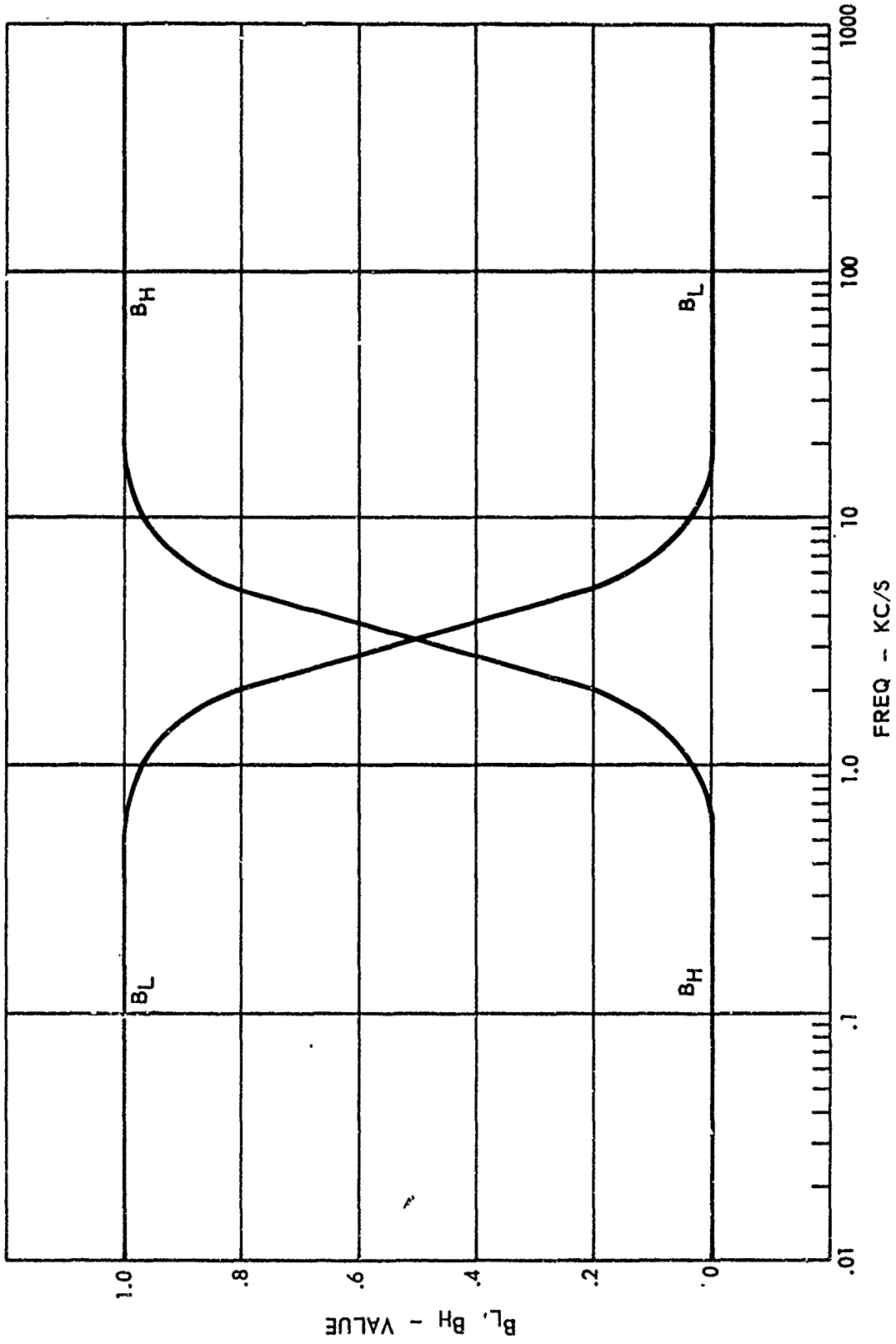


Figure 2. Frequency Dependent Weighting Factors.

Equation (7) is plotted versus frequency for averaged deep-ocean values of temperature, pressure, and salinity in figure 3. Included for comparison are the curves of Marsh and Schulkin, Thorp, Sheehy and Halley, and Leroy. The curve predicted by eq. (7) is seen to represent a reasonably good fit to the experimental data over the entire frequency range considered. In order to show the effects of temperature, salinity, and pressure, computations were carried out using eq. (7) and varying each of these parameters while holding the others constant. The results of these computations are shown in figures 4 and 5. Figure 4 shows the large effect of temperature at higher frequencies, and the insensitivity to temperature at the lower frequencies. Figure 5 shows the very small effect of pressure on the absorption coefficient, where the pressure of 125 atmospheres corresponds to a depth of 4000 feet. The effect of salinity has not been shown since its small effect could not be recognized on a graph of this size. For all practical purposes the effects of salinity and pressure are so small that they may be neglected, in which case we can write a simplified version of eq. (7):

$$\alpha = \frac{1.776f^{1.5}}{32.768+f^3} + \frac{1}{1+32.768/f^3} \cdot \left(\frac{.65053f_t^2}{f^2+f_t^2} + \frac{.026847f_t^2}{f_t} \right) \text{dB/kyd} \quad (8)$$

To derive a theoretically correct expression for α would require both new experiments and new theories. Equations (7) and (8) will give a reasonably good fit to available data, and include the important effects of the environment. Thus, they seem to represent the best available expressions for use in sonar range-prediction calculations. One of the principle advantages of eq. (7) is the smooth transition from an expression depending only on frequency, to one which depends on frequency, temperature, pressure, and salinity. One area of possible concern is that very little correction is provided for variations in temperature, pressure, and salinity at low frequencies; however, there is apparently no data available upon which to base such corrections. Indeed, it may be that at low frequencies α does not depend appreciably on these variables.

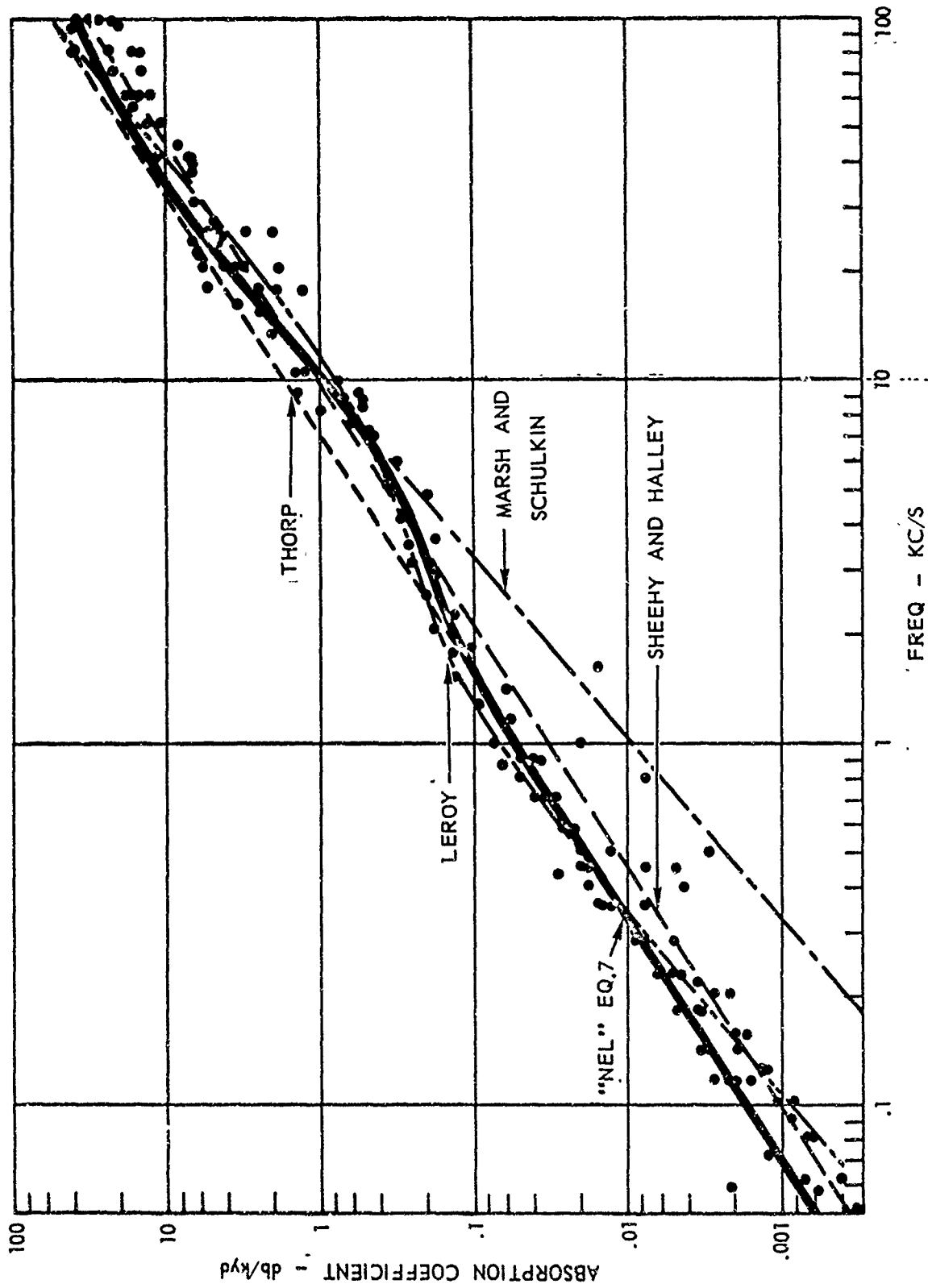


Figure 3. Comparison of Absorption Coefficients Including New "NEL" Curve, Temperature = 40° F, Salinity = 35 ‰, Pressure = 125 ATM.

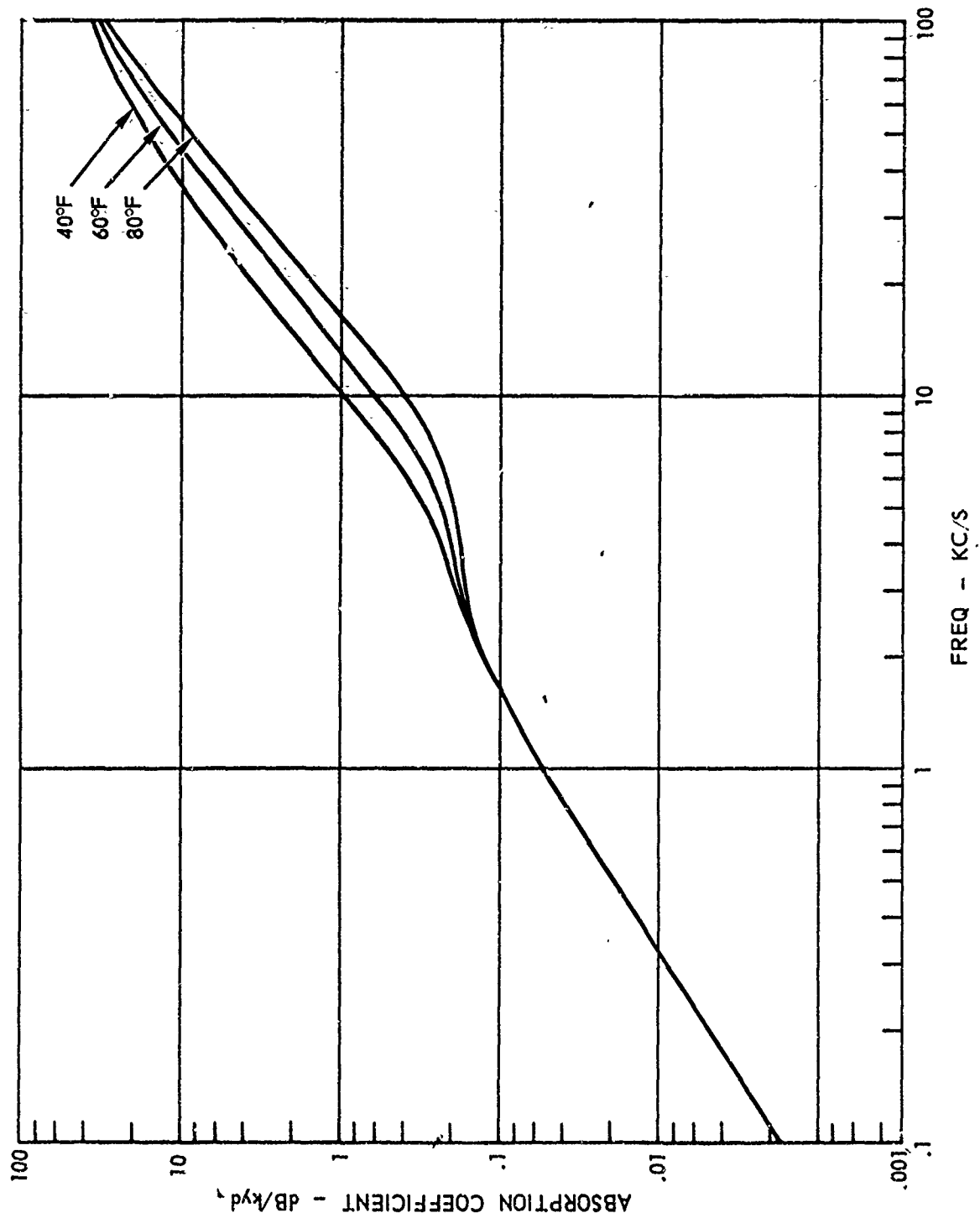


Figure 4. Change in Absorption Coefficient with Temperature "NEL"
Equation 7, Pressure = 125 ATM, Salinity = 35 ‰.

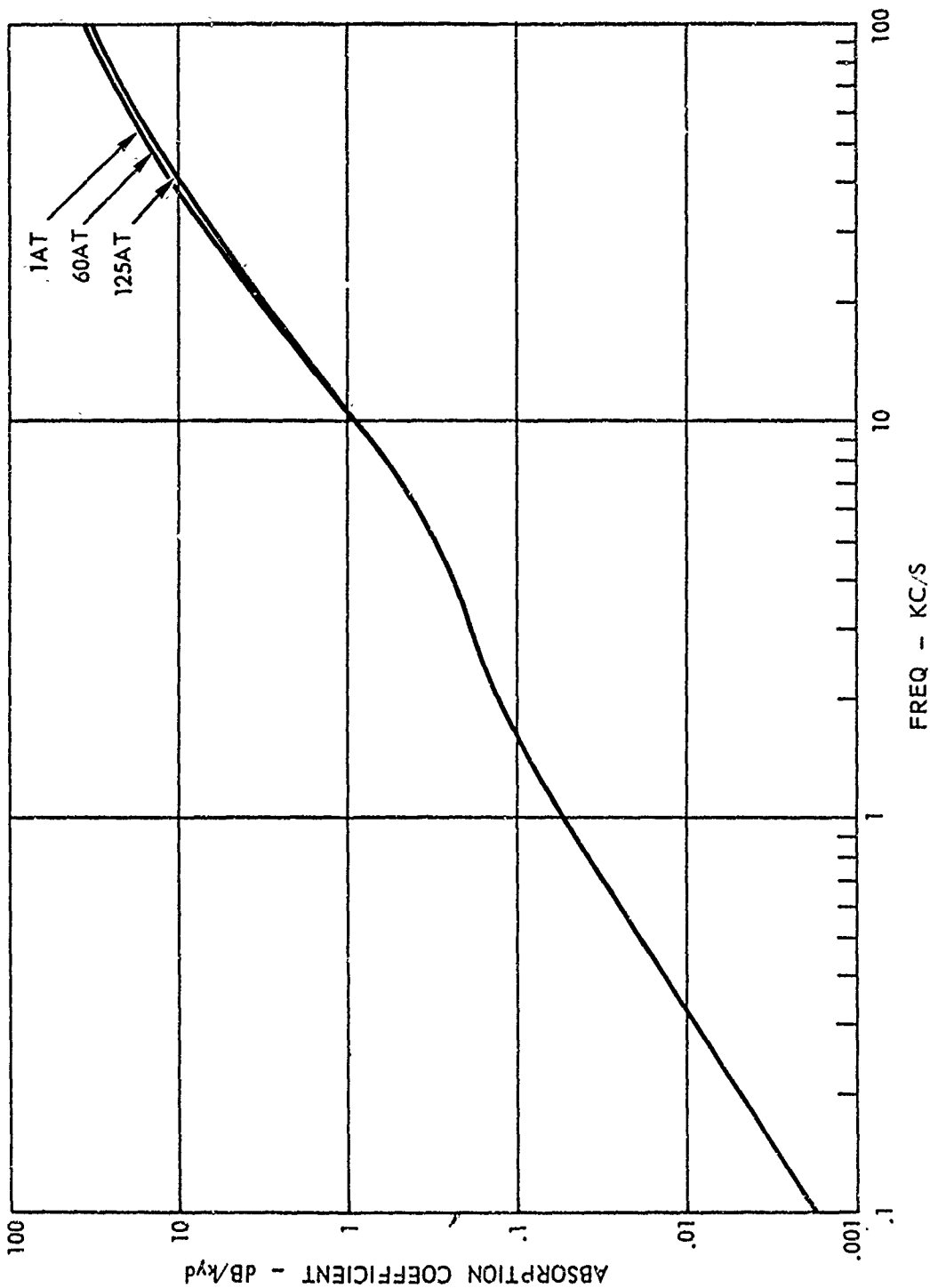


Figure 5. Change in Absorption Coefficient with Pressure "NEL" Equation 7, Temperature = 40° F, Salinity = 35 ‰.

CONFIDENTIAL

Equations (7) and (8) obviously do not represent new physical information. They do represent a practical combination of existing expressions appropriate for use in sonar range prediction.

PRACTICAL CONSIDERATIONS:

The following sections will describe an analysis carried out to determine how the value of the absorption coefficient can affect sonar detection ranges. A primary interest was in determining the magnitude of possible errors in detection range occurring when one or another of the alternative absorption loss expressions is used. In this analysis we will use the terms "NEL" eq. (7) and "NEL" eq. (8) to identify the new absorption coefficient expressions. "NEL" eq. (8) is presently being incorporated into all sonar system performance prediction models under the control of NEL Code 3110D. These prediction models are those which will be used for all official sonar system performance predictions carried out by the Navy Electronics Laboratory.

The first step in this analysis will be to place realistic bounds on possible sonar detection ranges. This is very important, since range errors will be a function of the detection ranges involved. The upper and lower bounds on detection range will be specified by placing upper and lower bounds on propagation loss, and on sonar system capability. We will focus our attention on active sonar systems, but the results of this analysis are equally applicable to passive sonar systems. The assumptions made are outlined below.

a. Sonar System Capability: System performance limits will be specified by figure of merit. Figure of merit for an active system is defined as the allowable two way propagation loss, for a zero dB target strength, which gives a 50% probability of detection at the sonar display. We will also define adjusted figure of merit as

$$F. O. M. (ADJUSTED) = F. O. M. + (TARGET STRENGTH)$$

In this analysis we will assume that all systems considered will have figures of merit which are between 180 and 200. A minimum value of 180 corresponds to a very good SQS-23 sonar. A sonar system having a figure of merit which is less than 180 will normally

CONFIDENTIAL

not give significant performance in bottom bounce, convergence zone, or other long range modes. A figure of merit of 180 is less than the measured figure of merit of the BQS-6 submarine sonar system, and it is also less than the expected figure of merit of the SQS-26 sonar system. These two systems represent the Navy's best present generation capability as far as long range sonar modes is concerned.

The maximum figure of merit of 200 is higher than that which will probably be achieved by the best SQS-26 sonar systems. A figure of merit higher than 200 will probably not exist in the fleet until the advent of the next generation sonar systems. Assuming a random aspect target strength of 15 dB, we can therefore arrive at the upper and lower bounds for adjusted figure of merit:

$$\text{F. O. M. (ADJUSTED)} = \left(\begin{array}{l} 195 \text{ MINIMUM} \\ 215 \text{ MAXIMUM} \end{array} \right)$$

b. Propagation Loss Limits: We can write the expression for propagation loss as

$$\text{PROPAGATION LOSS} = \text{SPREADING LOSS} + \text{BOUNDARY LOSSES} + \text{ABSORPTION LOSS}$$

The expressions which we select for maximum and minimum propagation loss should be simple, involve a minimum of terms, and predict losses which are consistent with those found in practice.

Selecting the minimum propagation loss expression is straightforward since we can assume cylindrical spreading and neglect boundary losses. In practice, one finds that cylindrical spreading will only occur at ranges greater than 500 yards, and that spherical spreading losses occur for shorter ranges. We can therefore write the expression for minimum two way propagation loss as:

$$\text{HMIN} = 114 + 20 \log(\text{RANGE}) + 2\alpha \cdot \text{RANGE} \quad (9)$$

where RANGE is the horizontal range in kyd. In practice losses under ducted conditions will very seldom, if ever, be less than this.

CONFIDENTIAL

In selecting the expression for maximum propagation loss we will assume spherical spreading losses at all ranges. We will also neglect boundary losses. This then gives for the maximum two way loss.

$$HMAX = 120 + 40 \log(RANGE) + 2\alpha \cdot RANGE \quad (10)$$

Throughout this analysis we will use horizontal range and slant range interchangeably. For ducted cases horizontal range is appropriate, while slant range is appropriate to non-ducted cases. In later computations we will always use horizontal range for purposes of simplification, and we will assume the resulting errors to be negligible.

It is apparent that the losses predicted by eq. (10) will be somewhat less than those usually experienced in the bottom bounce mode, since we are neglecting bottom reflection losses. Expression (10) will therefore predict losses which cover the middle ranges, and approach those found in the bottom bounce mode.

As we will shortly see, equations (9) and (10), when combined with the specified figure of merit limits, will bracket all values of detection range pertinent to this analysis.

The detection range error analysis was carried out by computing propagation loss as a function of range with frequency as a parameter. These computations were carried out using the absorption coefficient expressions of Marsh and Schulkin, Thorp, Sheehy and Halley, and "NEL" eq.(7). We have not made comparisons using Leroy's expression since it has not found extensive application in range prediction. These computed propagation loss values were used with the specified figure of merit limits to determine the variation in detection range.

The basic principle of the analysis is illustrated in figures 6 and 7, which show two way propagation loss as a function of range for several selected frequencies. Values were actually computed for many frequencies from very low to very high values, but for clarity we have shown data for only three frequencies. Figure 6 illustrates the minimum loss case, and figure 7 shows

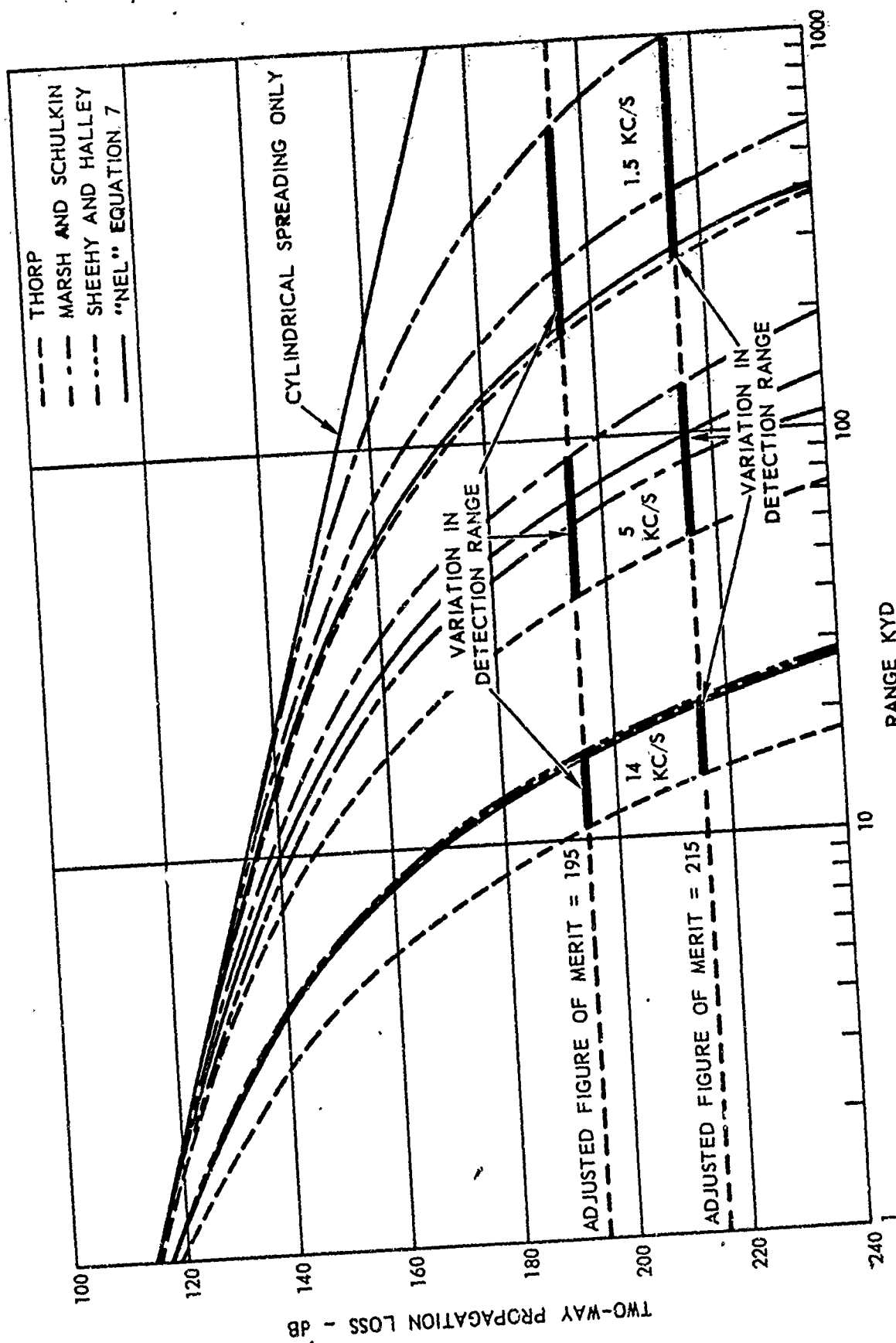


Figure 6. Two-Way Loss vs Range, Cylindrical Spreading, T = 40° F, P = 125 ATM, S = 35°/oo.

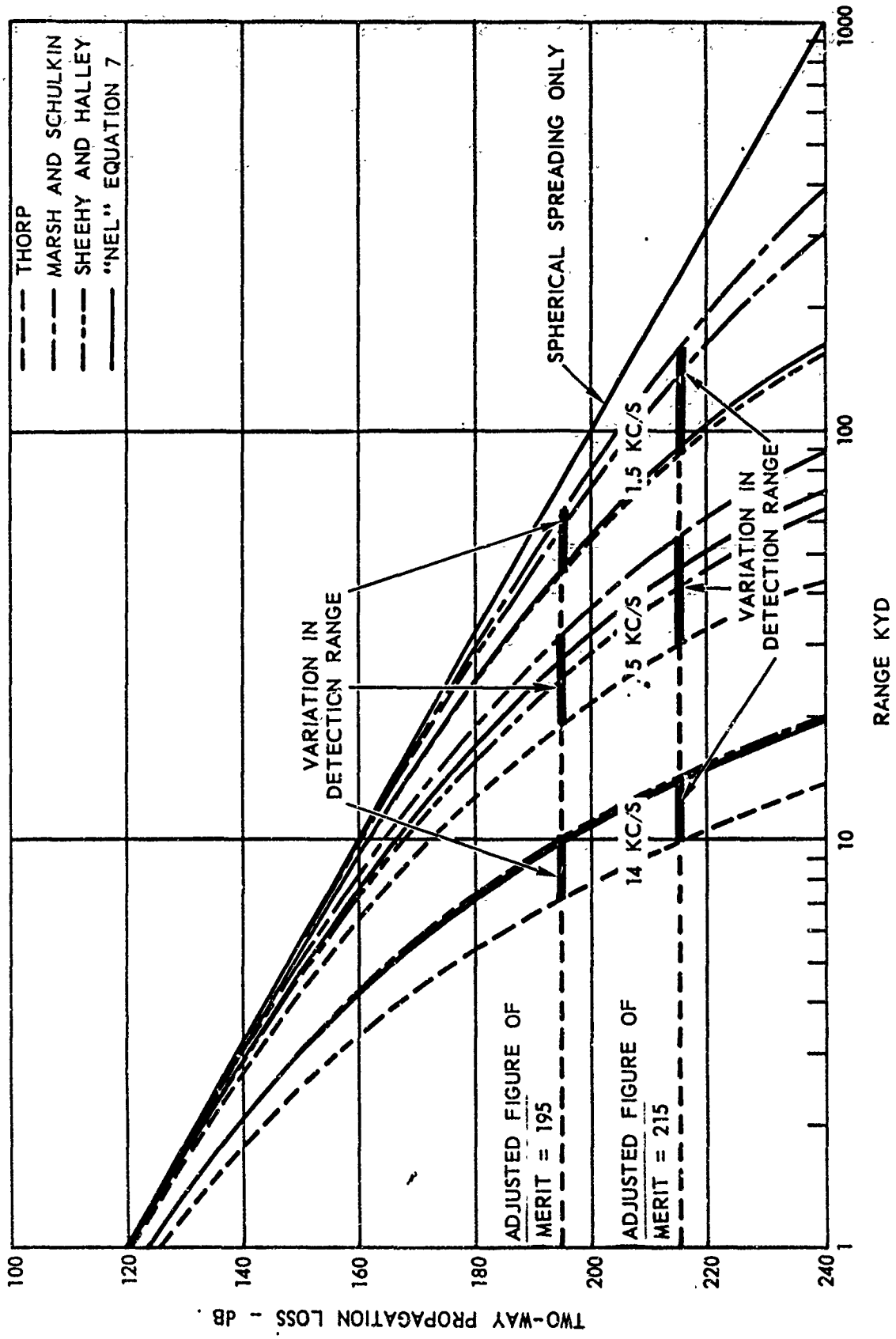


Figure 7. Two-Way Loss vs Range, Spherical Spreading, $T = 40^{\circ} F$,
 $P = 125 \text{ ATM}$, $S = 35 \text{ } \mu\text{o}$.

CONFIDENTIAL

the maximum loss case. On each of these curves horizontal lines corresponding to the specified minimum and maximum figures of merit are shown. The intersection of each of the propagation loss curves and the figure of merit lines determines the detection range for that particular case. The variation in detection range due to using the various absorption coefficient expressions is then represented by the heavy horizontal line segments.

Figures 6 and 7 collectively picture the combined effects of the most optimistic and most pessimistic sets of assumptions. Both figures illustrate the fact that detection range error as a percentage of detection range is not critically dependent upon the assumed figures of merit, since shifting the figure of merit lines up or down several dB does not have a large effect. Also, adding a fixed loss to the propagation loss curves, corresponding to added boundary losses, does not appreciably affect the percentage error in detection range. This is particularly true for the maximum loss curves which would normally be associated with the higher boundary losses.

Figures 6 and 7 are presented to illustrate the general approach used. Actual values of detection range for the various conditions and for many frequencies were calculated on an NEL Univac 1230 computer using a modified Newton's method. The initial analysis was carried out using averaged deep ocean values of temperature, pressure, and salinity. Figures 8, 9, 10, and 11 show the computed detection ranges for each combination of propagation loss and figure of merit. These figures show the predicted detection ranges using various absorption coefficient expressions.

Figure 8 corresponds to low figure of merit and high propagation losses. Subsequent figures show results for other combinations of figure of merit and propagation loss which give longer detection ranges. Figure 8 shows the shortest detection ranges while figure 11 shows the longest detection ranges. These figures illustrate the fact that at both long and short ranges, and at low and high frequencies, the actual detection ranges can vary appreciably when using different expressions for the absorption loss coefficient.

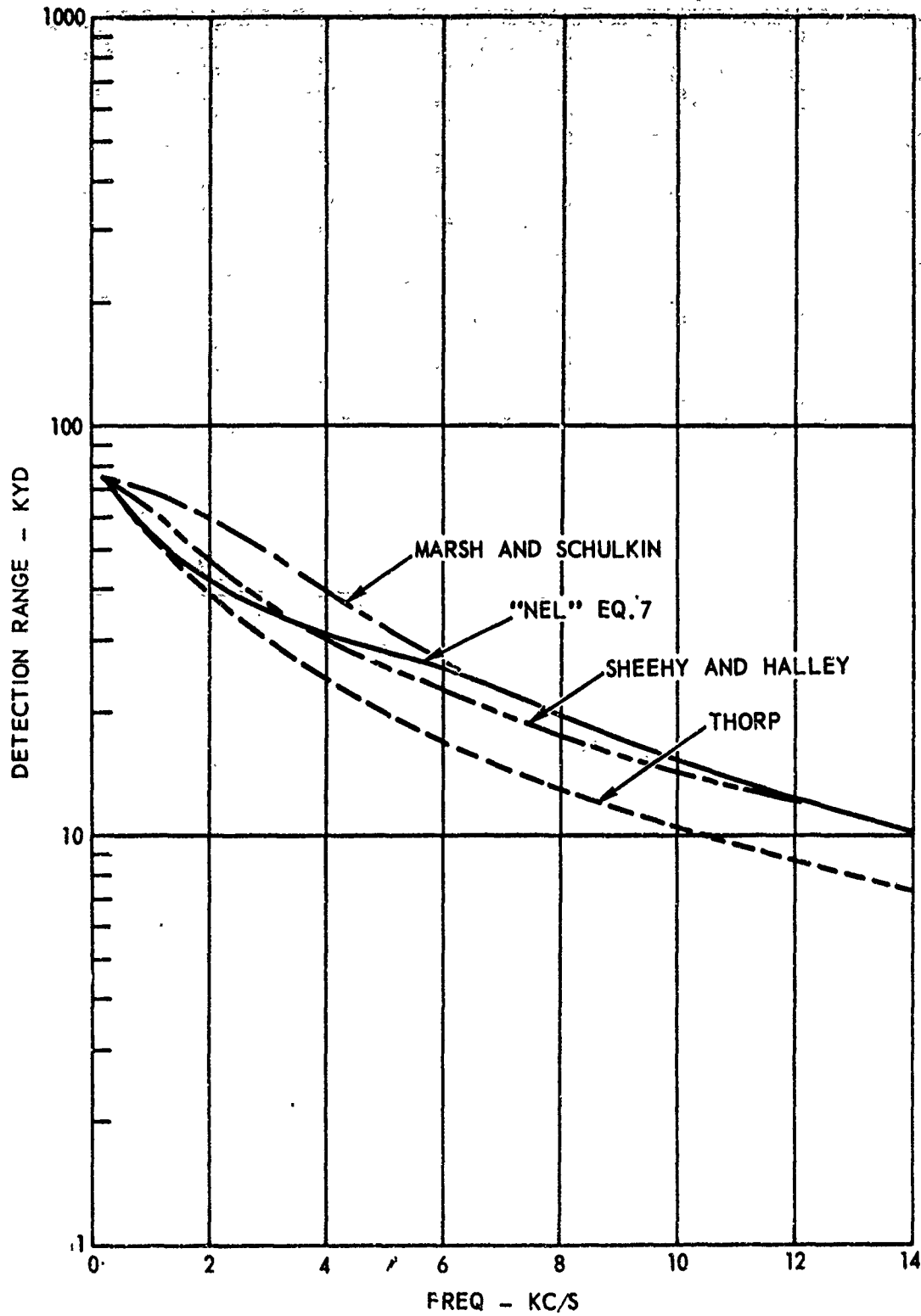


Figure 8. Detection Range vs Frequency, Spherical Spreading, Adjusted F. O. M. = 195, Temperature = 40° F, Salinity = 35‰, Pressure = 125 ATM.

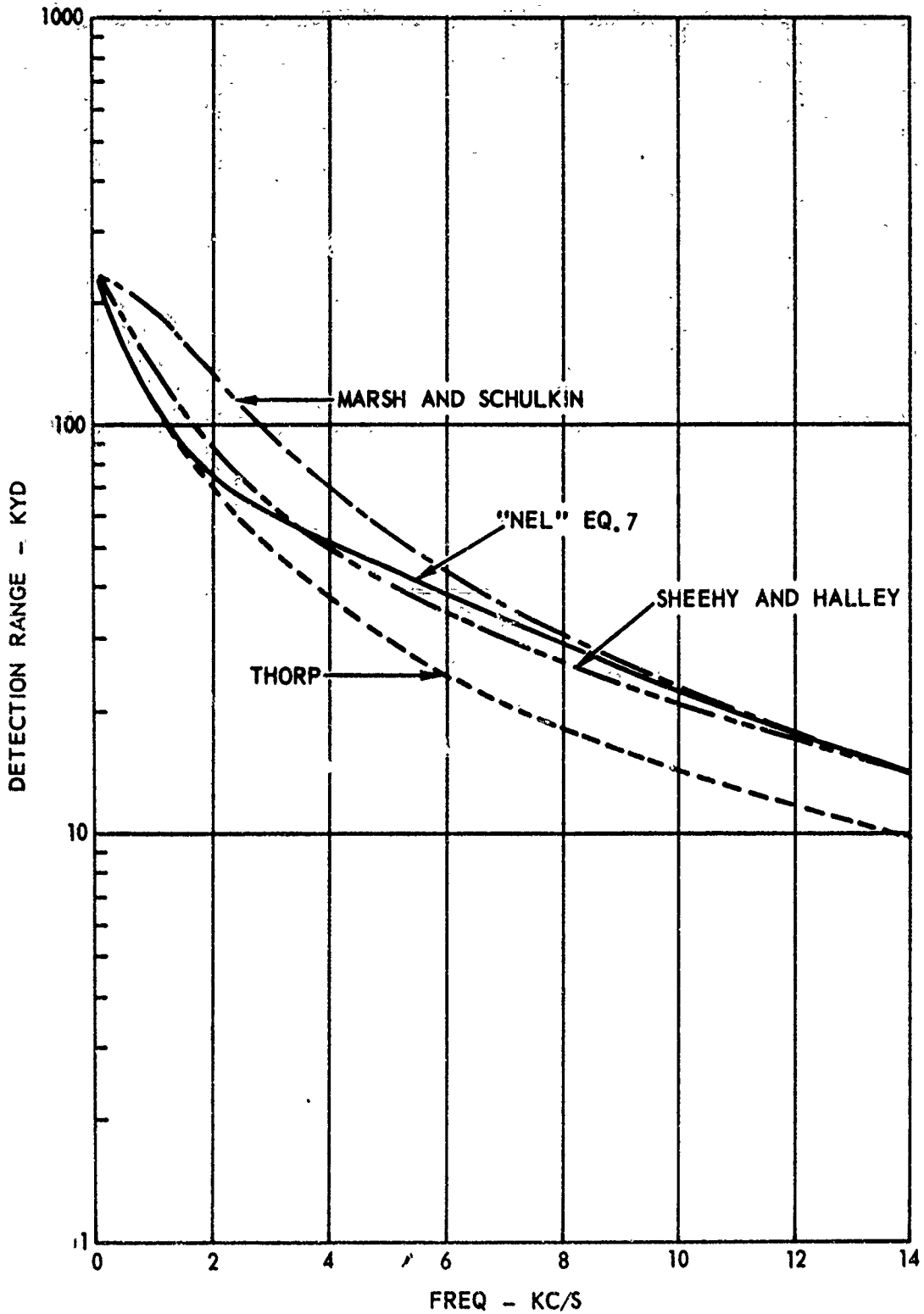


Figure 9. Detection Range vs Frequency, Spherical Spreading, Adjusted F.O.M. = 215, Temperature = 40° F, Salinity = 35‰, Pressure = 125 ATM.

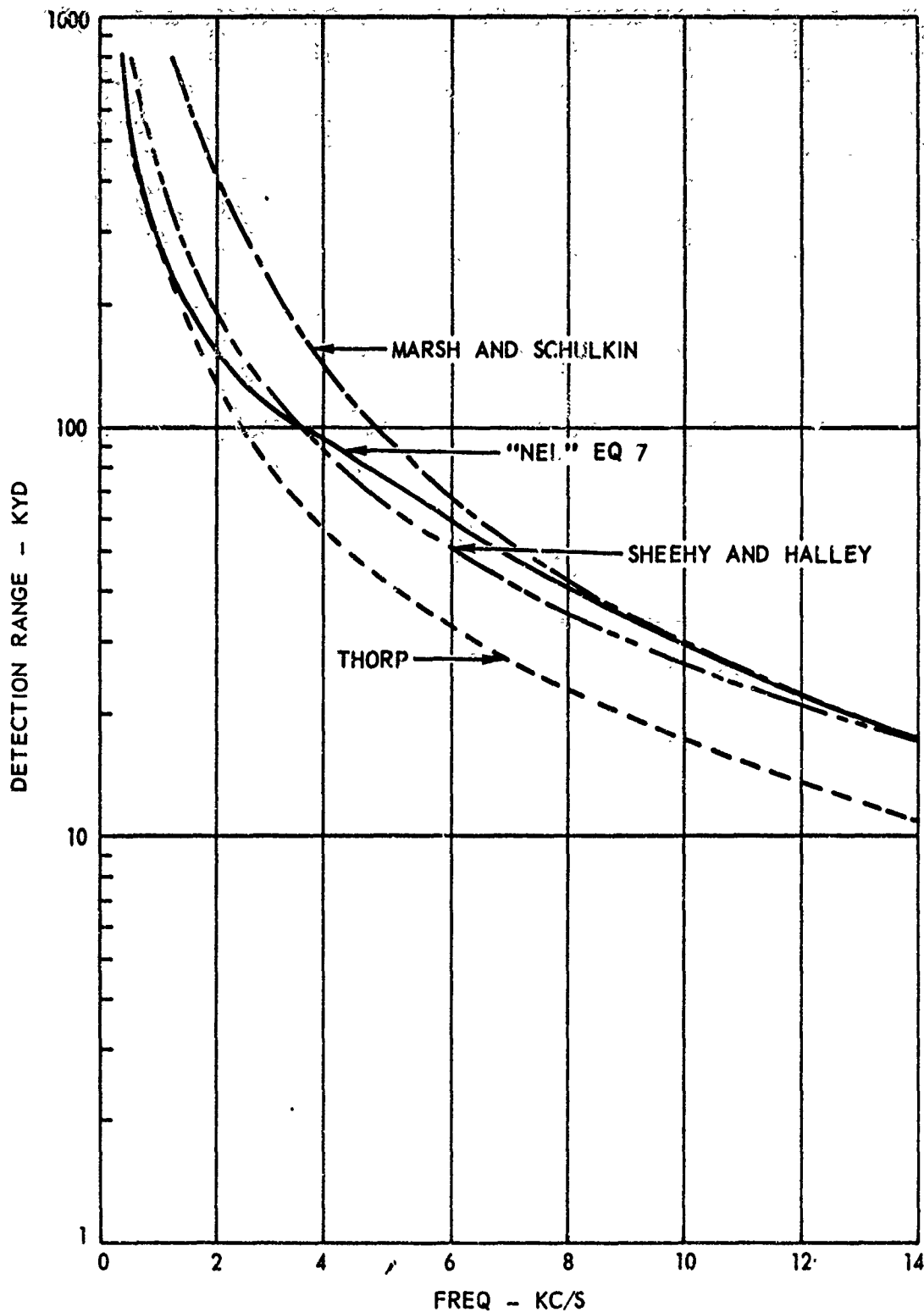


Figure 10. Detection Range vs Frequency, Cylindrical Spreading, Adjusted F. O. M. = 195, Temperature = 40° F, Salinity = 35‰, Pressure = 125 ATM.

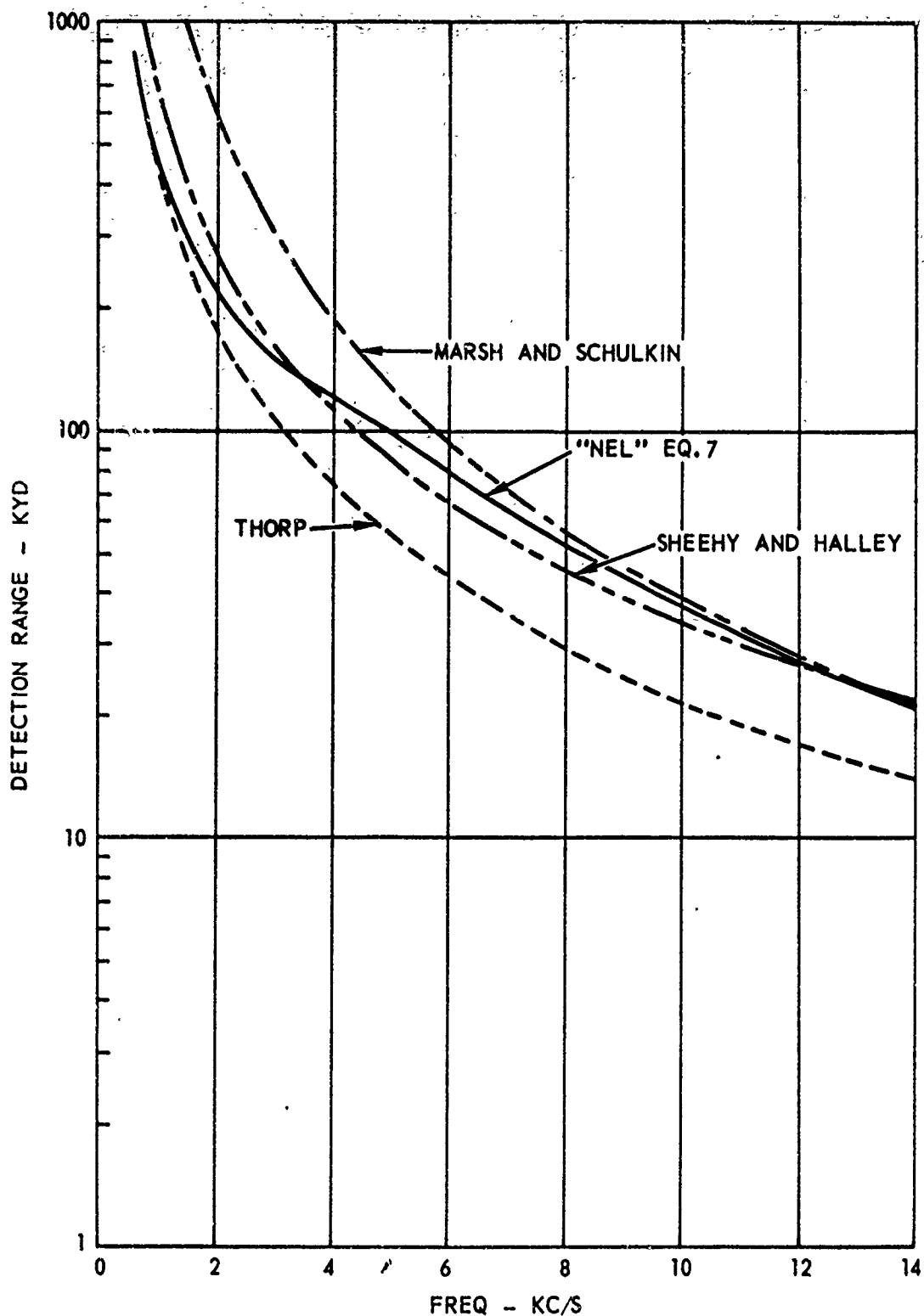


Figure 11. Detection Range vs Frequency, Cylindrical Spreading, Adjusted F. O. M. = 215, Temperature = 40° F, Salinity = 35‰, Pressure = 125 ATM.

CONFIDENTIAL

The percent detection range error was selected as the most reasonable basis for evaluating each of the absorption coefficients.* Since the absorption coefficients represented by "NEL" eqs. (7) and (8) appear to be the most nearly exact over the wide frequency range of interest, we have assumed that correct detection ranges are computed when they are used. This normalizes the error with respect to the values predicted by "NEL" eqs. (7) and (8).

Percent detection range error was then computed for the four combinations of figure of merit and propagation loss, using various absorption coefficient expressions. The results are plotted in figure 12 which shows the extreme maximum and minimum errors which can occur. The maximum error corresponds to the adjusted F. O. M. value of 215 with cylindrical spreading, and is shown by the solid lines. The minimum error corresponds to an adjusted F. O. M. of 195 with spherical spreading, and is shown by the dashed lines. We can see from figure 12 that Thorp's expression gives small error at low frequencies, while Marsh and Schulkin's expression gives small error at high frequencies. This is expected since they respectively make up the low and high frequency parts of "NEL" eq. (7).

Note that the use of Thorp's absorption expression can give detection range errors of from 20 to 30% at 3.5 kc/s. This results from the fact that the expression of Thorp is a poor fit to the data near 3.5 kc/s. Also note that the absorption coefficient of Sheehy and Halley predicts zero error near 3.5 kc/s and in fact gives smaller errors than the expression of Thorp for all frequencies above 2.5 kc/s.

Figure 12 illustrates the sacrifice in detection range accuracy which can result from using some of the commonly used absorption expressions over frequency ranges where they are not applicable.

*The use of the term "error" does not imply errors on the part of the authors who proposed the various expressions, since in many cases the expressions have been used here outside of their originally intended applicable frequency ranges. Thus, in many cases, the errors calculated are those which would be incurred by persons using the expressions where they are not applicable.

CONFIDENTIAL

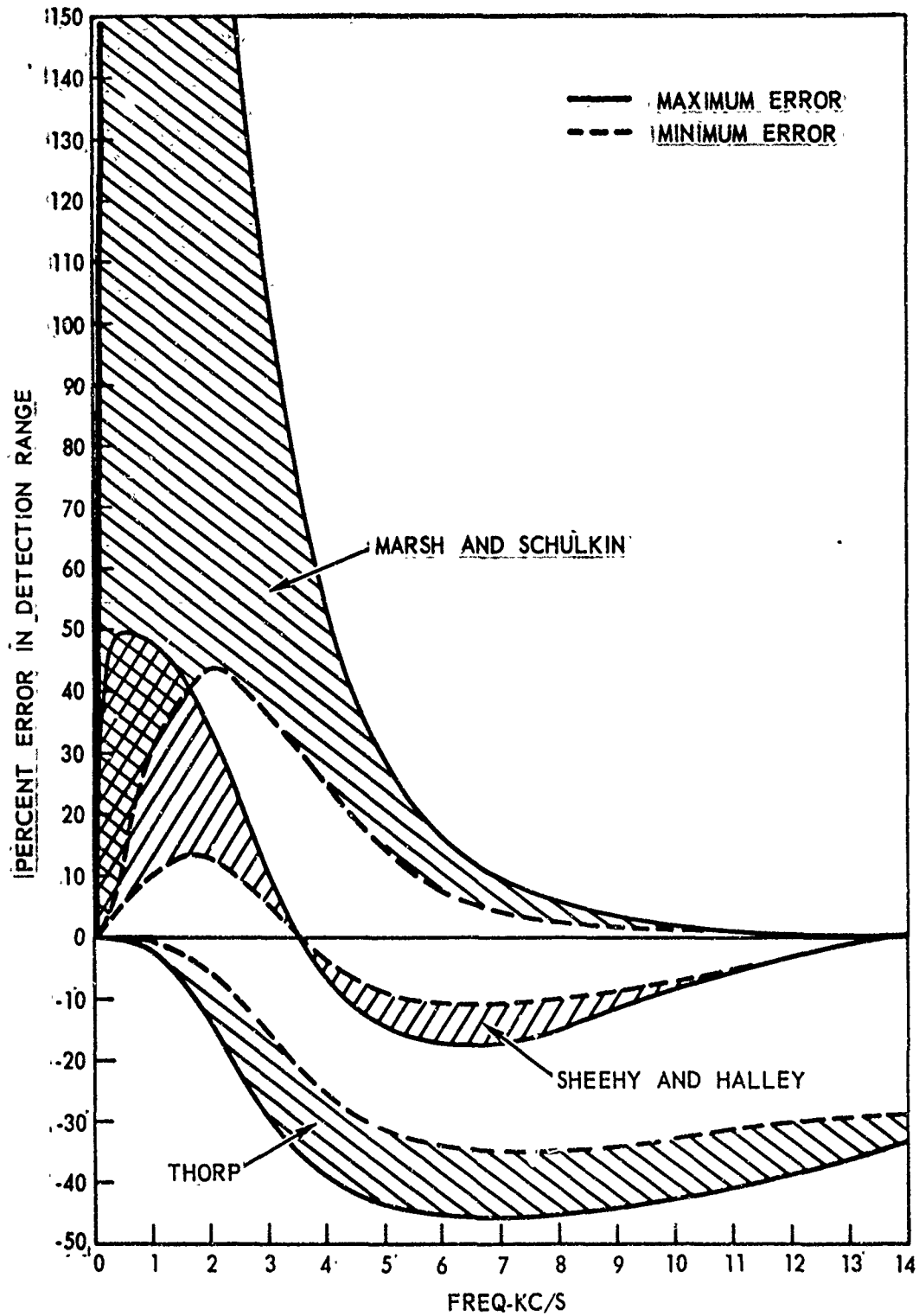


Figure 12. Percent Error in Detection Range vs Frequency, Range of Errors, Temperature = 40° F, Salinity = 35‰, Pressure = 1 ATM.

CONFIDENTIAL

Additional errors can result from use of absorption coefficient expressions which are temperature insensitive at the higher operating frequencies. The effects of temperature have been computed using each of the absorption coefficients. Computations were carried out and plotted for 40, 60, and 80 degrees F and for both good and poor sonar performance. Results from these computations are plotted in figures 13, 14, 15, 16, 17, and 18.

Referring to these figures, one can see that significant additional errors can result from the use of Thorp, or Sheehy and Halley at higher frequencies with warmer water temperatures.

In order to illustrate the importance of including temperature effects at higher frequencies, a series of calculations were carried out using "NEL" eq. (7). Propagation loss was computed for three water temperatures and for constant pressure and salinity. The results of these calculations are plotted in figures 19 and 20 for various combinations of spreading loss and figure of merit. It can be seen that neglecting water temperature can lead to appreciable errors in detection range at frequencies above 3 kc/s. At the higher frequencies temperature variations can lead to range errors as high as 30 kyd, with relative errors approaching 50%.

APPLICABILITY TO PROPAGATING MODES:

As a last part of this analysis it seems worthwhile to discuss each of the common sonar propagation modes in the framework of this error analysis.

a. Surface Channel: Surface channel performance depends greatly upon layer depth, frequency, and ocean surface conditions. For low sea states and deep channels very long ranges can be achieved, limited only by cylindrical spreading and absorption losses. For high sea states and for shallow channels, propagation losses can increase to the point where they will equal or exceed the maximum loss values used in this analysis.

Surface channel performance in almost all cases will fall within the performance limits of this analysis. Good long range surface channel performance is possible from frequencies as low as 500 cycles up to frequencies of 14 kc/s and above. Low frequency performance can be very important for passive systems operating in northern forward areas.

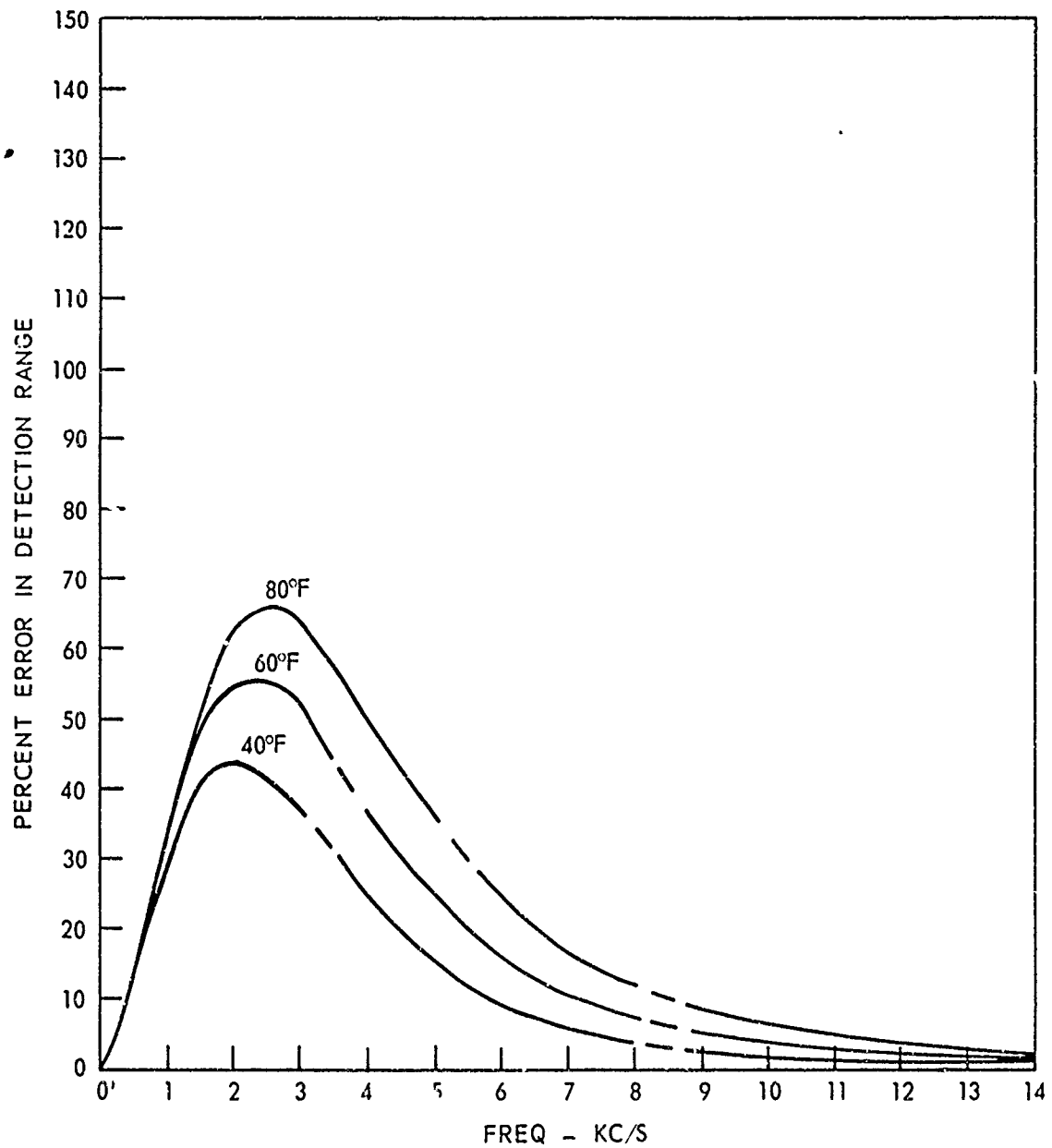


Figure 13. Percent Error in Detection Range vs Frequency, Absorption Coefficient of Marsh and Schulkin, Spherical Spreading, Adjusted F. O. M. = 195, Salinity = 35‰, Pressure = 1 ATM.

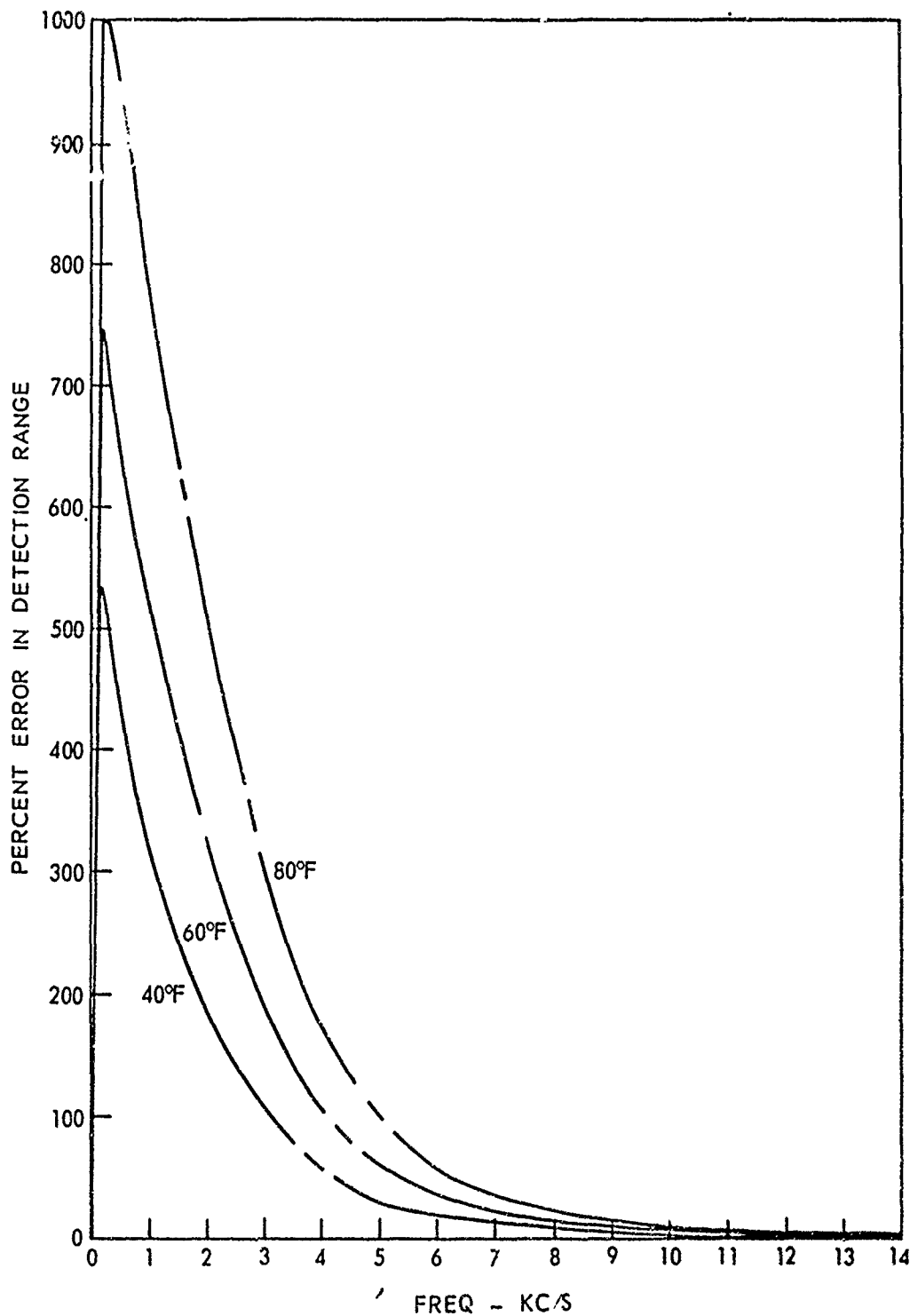


Figure 14. Percent Error in Detection Range vs Frequency, Absorption Coefficient of Marsh and Schulkin, Cylindrical Spreading, Adjusted F.O.M. = 215. Salinity = 35‰. Pressure = 1 ATM.

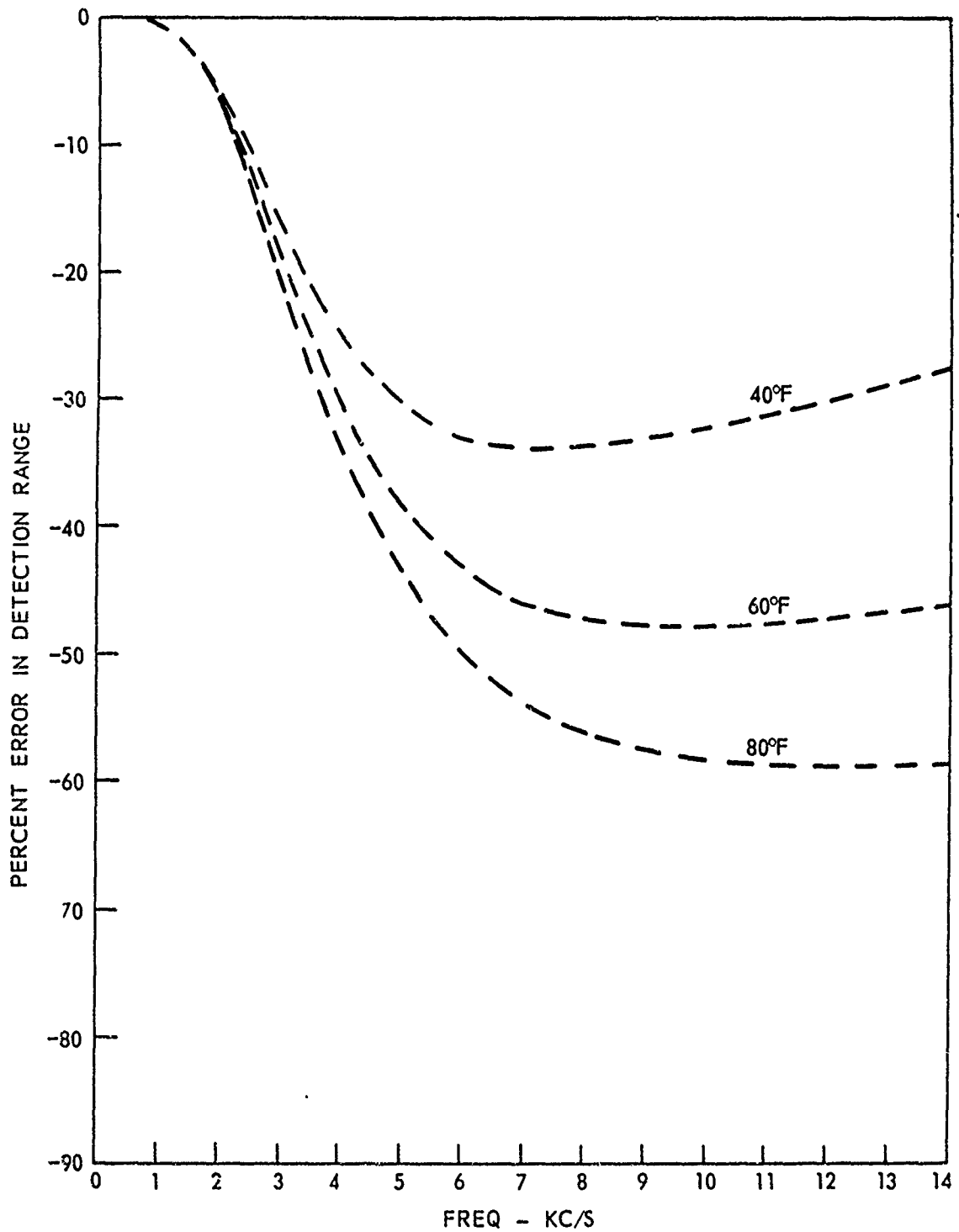


Figure 15. Percent Error in Detection Range vs Frequency, Absorption Coefficient of Thorp, Spherical Spreading, Adjusted F. O. M. = 195, Salinity = 35‰, Pressure = 1 ATM.

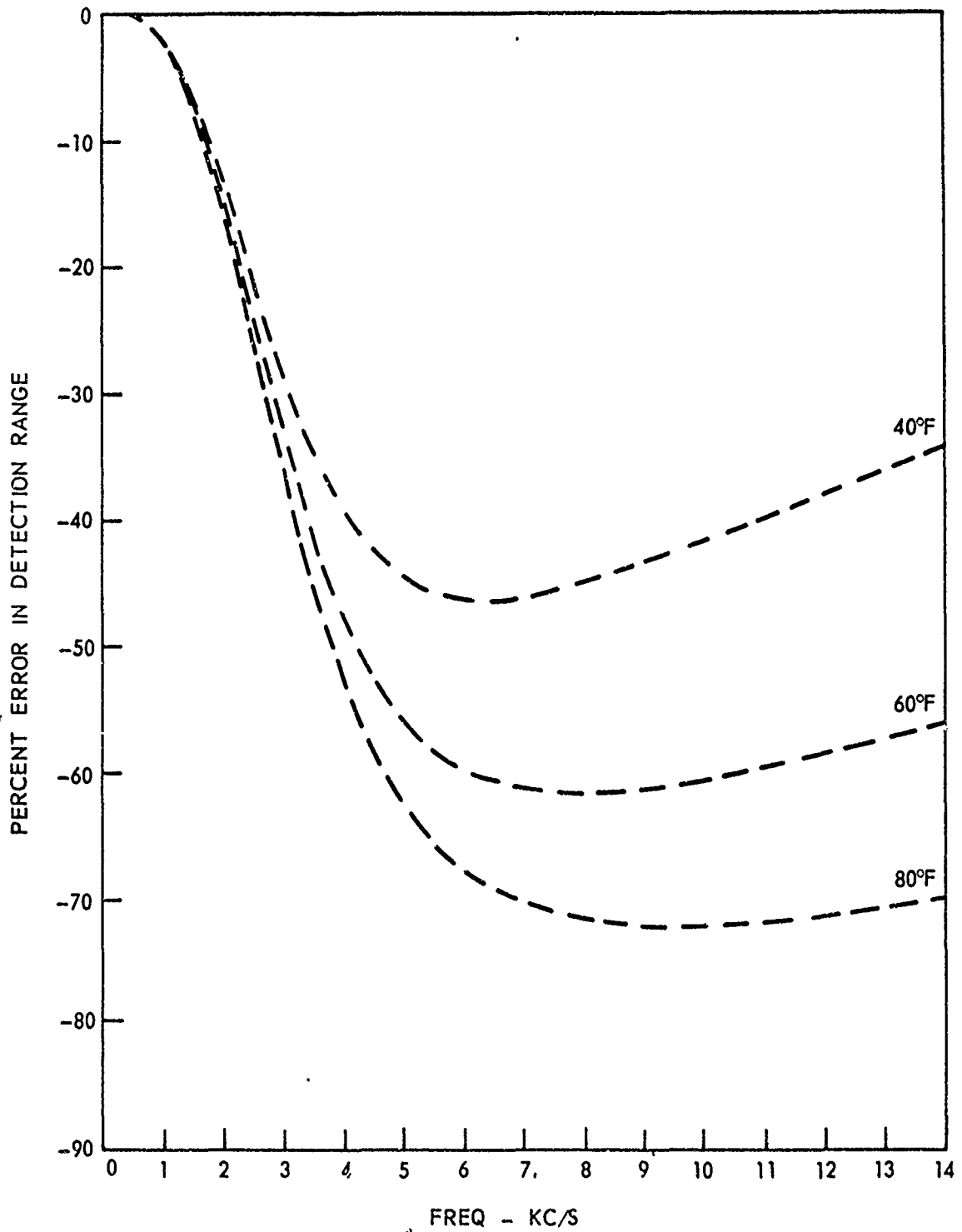


Figure 16. Percent Error in Detection Range vs Frequency, Absorption Coefficient of Thorp, Cylindrical Spreading, Adjusted F.O.M. = 215, Salinity = 35‰, Pressure = 1 ATM.

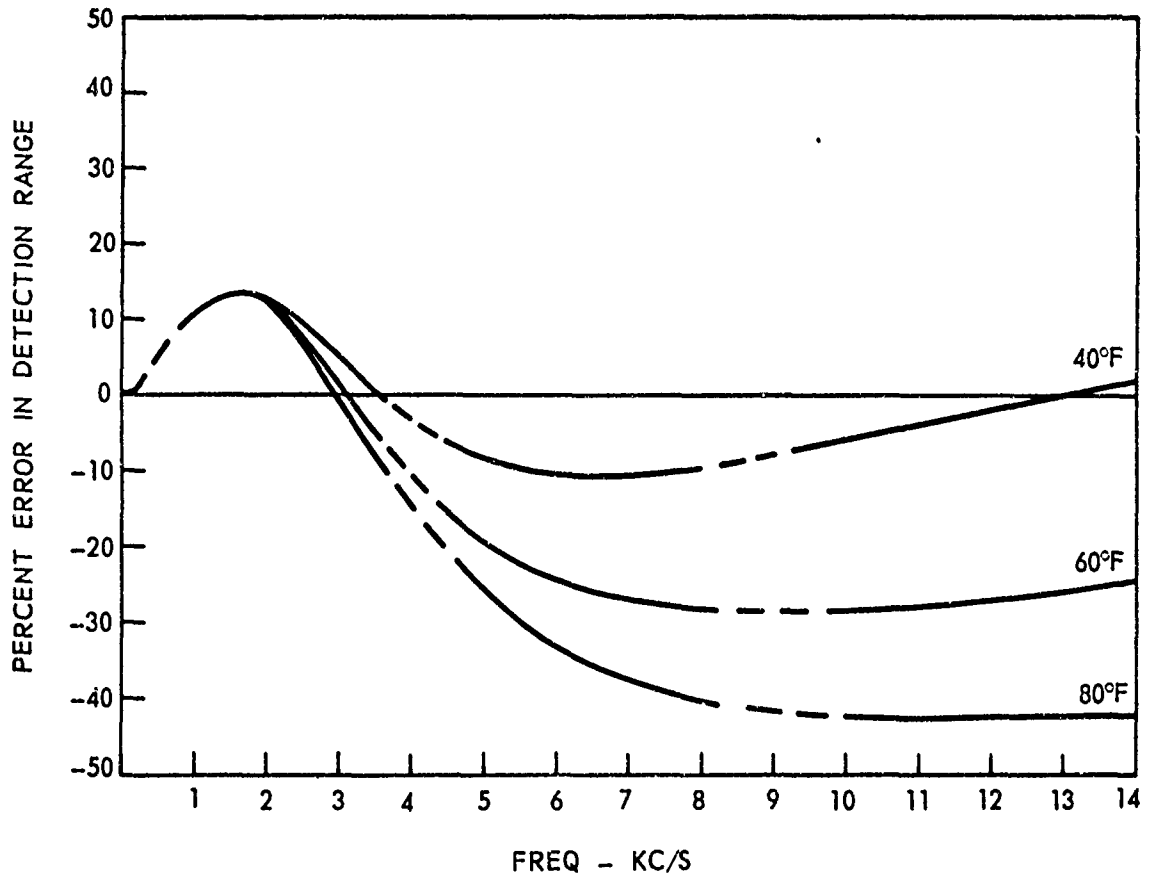


Figure 17. Percent Error in Detection Range vs Frequency, Absorption Coefficient of Sheehy and Halley, Spherical Spreading, Adjusted F.O.M. = 195, Salinity = 35‰, Pressure = 1 ATM.

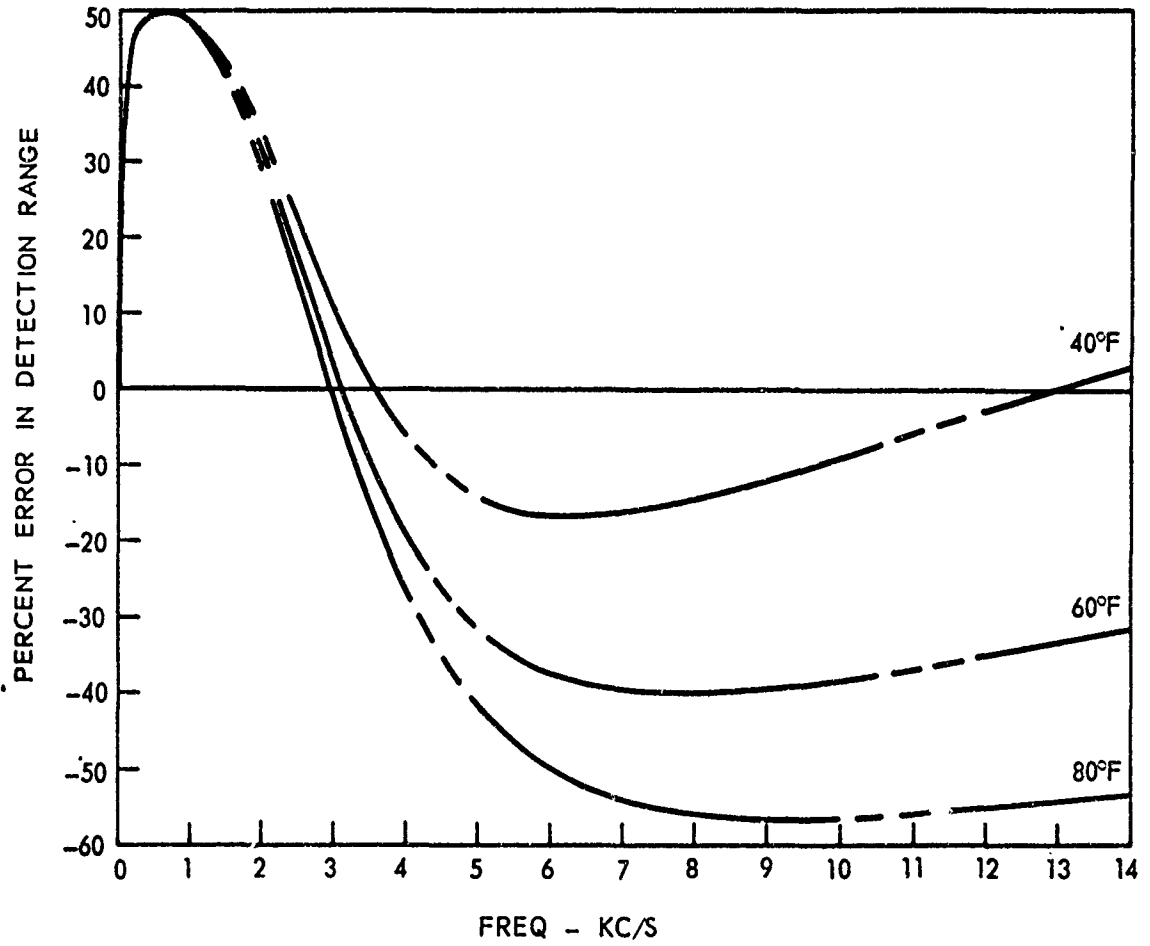


Figure 18. Percent Error in Detection Range vs Frequency, Absorption Coefficient of Sheehy and Halley, Cylindrical Spreading, Adjusted F.O.M. = 215, Salinity = 35‰, Pressure = 1 ATM.

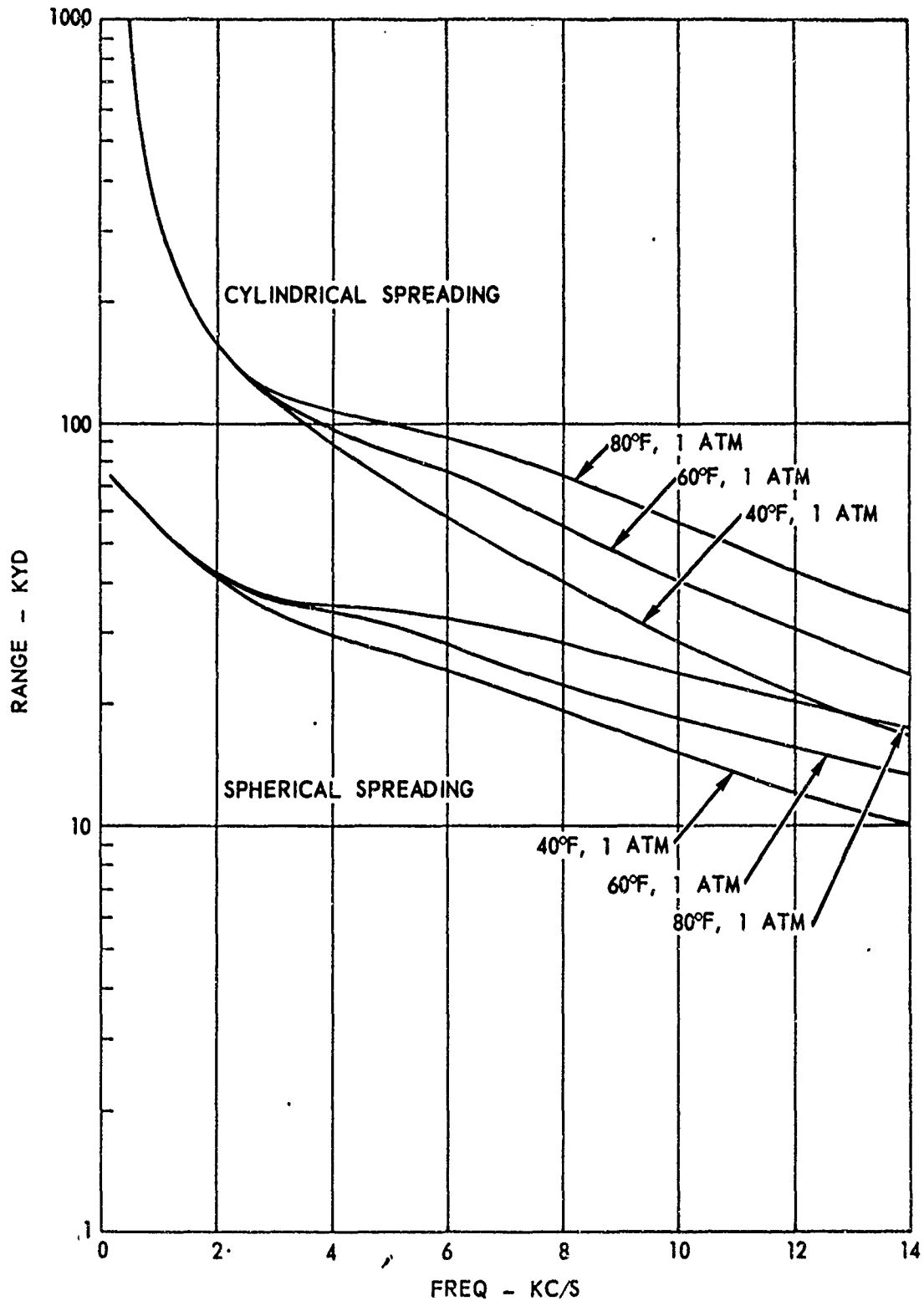


Figure 19. Detection Range vs Frequency, "NEL" Eq. 7, Absorption Coefficient, Adjusted F.O.M. = 195.

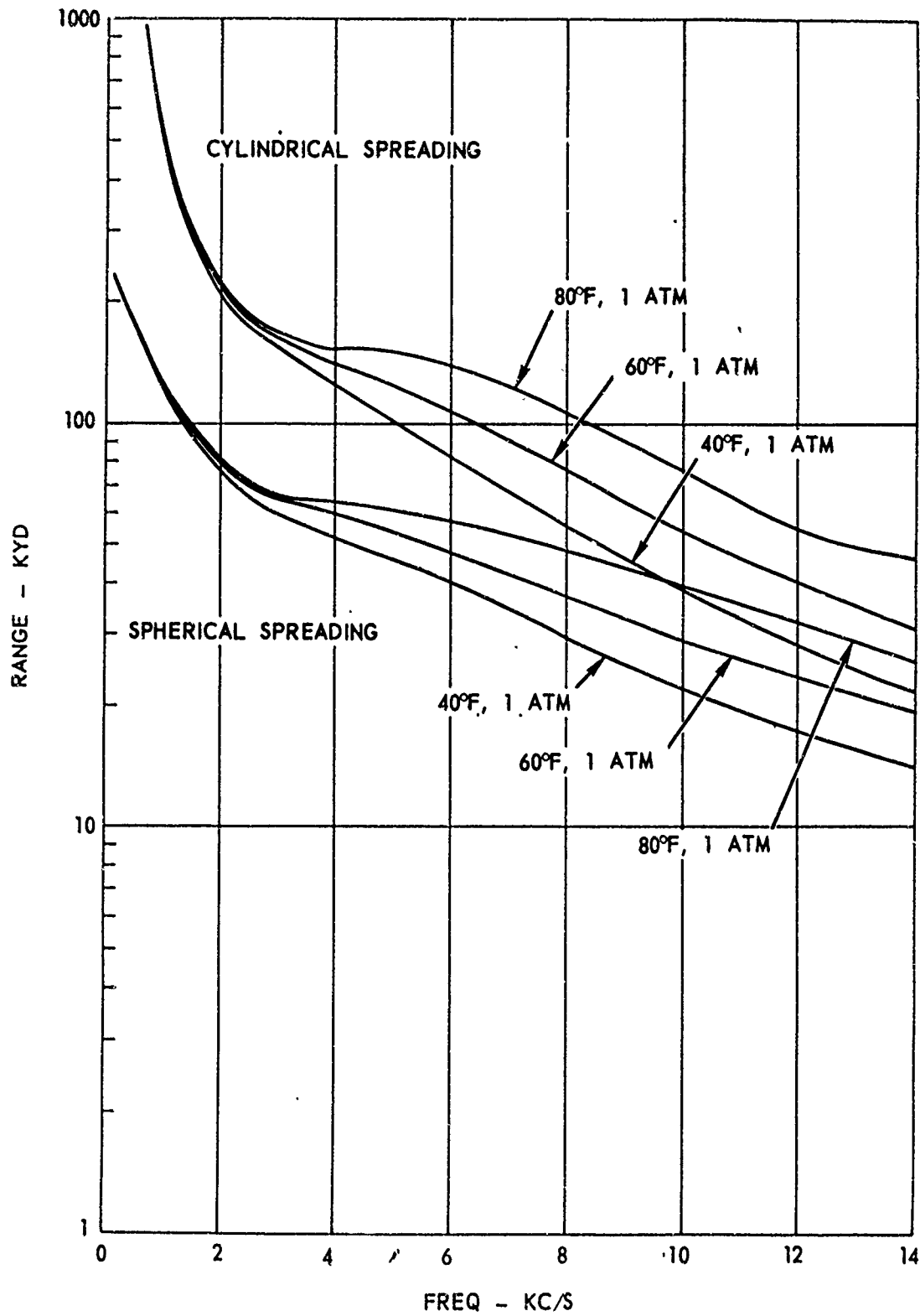


Figure 20. Detection Range vs Frequency, "NEL" Eq. 7, Absorption Coefficient, Adjusted F.O.M. = 215.

CONFIDENTIAL

The water temperature associated with surface channel operation can be quite variable since it will be greatly influenced by local weather conditions and surface currents.

It is therefore apparent that operation in the surface channel mode can involve the full gamut of temperature variations and performance limits over most of the frequency range considered. Under poor performance, short-range detection conditions, absorption losses will be small; but when conditions allow surface channel detection ranges within those shown in this analysis, one must accept appreciable errors when using inappropriate absorption loss expressions.

b. Shallow Water: Several types of shallow water propagation are possible, depending upon the sound velocity profile, and the ocean surface and bottom characteristics. Since propagation is bounded, spreading loss is cylindrical, but boundary losses can be appreciable under some conditions. In practice, propagation losses will generally fall within the limits which apply to the surface channel cases. Shallow water modes will also involve considerable variation in water temperature. The resulting detection ranges can be very long or very short. When detection ranges fall within the limits considered in this analysis, one can expect substantial errors if the correct absorption loss expression is not used.

c. Bottom Bounce: Bottom bounce performance can vary from the minimum to the maximum detection ranges postulated in the error analysis. Shorter detection ranges will be associated with a single bottom reflection, while longer ranges will involve multiple bottom reflections. Temperature effects will be less important in the bottom bounce mode since it is a deep water path involving nearly constant water temperature.

The effects of absorption loss will be somewhat diminished by the effects of bottom loss which will almost always equal or exceed absorption losses. Added bottom losses will reduce the actual detection range error but will have little effect on the percent detection range errors as noted in figures 6 and 7.

d. Convergence Zone: Convergence zone propagation loss at the zone positions will fall near the minimum values shown in

CONFIDENTIAL

this analysis. Since zone range is fixed by ray optics the effects of using the various absorption loss expressions cannot be measured in terms of detection range, but must instead be measured in terms of propagation loss. This effect is best illustrated by referring back to figure 6. If we consider the 1.5 kc/s curves, and assume a zone at approximately 60 kyd, we can see that the two way propagation loss variation between predictions using Sheehy and Halley, and using Thorp is approximately 5 dB. Predictions using "NEL" eq. (7) and Thorp are within 1 dB of each other. For the second convergence zone these errors would be multiplied by two giving 10 dB difference where we had 5 before. It is therefore apparent that considerable error can result from use of incorrect absorption expressions, particularly for second and third zones. Again, as with bottom bounce, the deep water character of the propagation paths reduces the sensitivity to water temperature.

e. SOFAR Paths: Deep refraction channels lead to the minimum propagation losses one can find. They are generally temperature insensitive, but due to the very long ranges involved the actual and percent errors can become appreciable.

SUMMARY AND CONCLUSIONS:

Using a linear, weighted combination of the expressions of Thorp, and Marsh and Schulkin, a new absorption coefficient has been developed which predicts the available experimental data and includes the effects of temperature, salinity, and pressure.

Based on a study of detection errors under typical sonar conditions, it was determined that significant propagation loss and detection range errors can result from the use of incorrect absorption loss expressions. These errors can occur for all sonar modes, and at all operating frequencies.

Clearly, the use of the Marsh and Schulkin absorption loss expression at low frequencies can lead to prohibitive errors. Also, the use of Thorp's absorption loss expression can give fairly large errors at higher frequencies, particularly when using near surface modes involving variable water temperatures. Sheehy and Halley's expression gives answers which have the least overall deviation from those of "NEL" eq. (7) when the entire frequency range is

~~CONFIDENTIAL~~
UNCLASSIFIED

considered. However, Sheehy and Halley's expression suffers from neglecting water temperature variations at higher frequencies when operating in near surface propagation modes.

UNCLASSIFIED
~~CONFIDENTIAL~~

~~CONFIDENTIAL~~

UNCLASSIFIED

REFERENCES:

1. M. Schulkin and H. W. Marsh, "Sound Absorption in Sea Water," JASA v. 34, pp. 864-865, June 1962.
2. W. H. Thorp, "Deep-Ocean Sound Attenuation in the Sub- and Low-Kilocycle-Per-Second Region," JASA v. 38, pp. 648-654, October 1965.
3. M. J. Sheehy and R. Halley, "Attenuation of Low-Frequency Sound," JASA v. 29, pp. 464-469, April 1957.
4. C. C. Leroy, Sound Attenuation Between 200 and 10,000 CPS Measured Along Single Paths, SACLANT ASW Research Centre, La Spezia, Italy, TR #43, September 1965.
5. J. G. Truxal, Control Engineers' Handbook, McGraw-Hill Book Co., N. Y., 1958, p. 4-23.

REVERSE SIDE BLANK

UNCLASSIFIED

~~CONFIDENTIAL~~

35